

Cell Chemical Biology, Volume 29

Supplemental information

**An antibody-based proximity labeling
map reveals mechanisms of SARS-CoV-2
inhibition of antiviral immunity**

Yuehui Zhang, Limin Shang, Jing Zhang, Yuchen Liu, Chaozhi Jin, Yanan Zhao, Xiaobo Lei, Wenjing Wang, Xia Xiao, Xiuyuan Zhang, Yujiao Liu, Linlin Liu, Meng-Wei Zhuang, Qingkun Mi, Chunyan Tian, Jianwei Wang, Fuchu He, Pei-Hui Wang, and Jian Wang

SUPPLEMENTAL INFORMATION

Figure S1. Correlation analysis of each sample of the proximity labelling experiments, Related to Figure 3.

Figure S2. Gene Ontology (GO) and pathway (Reactome) analysis of the proximal proteins of SARS-CoV-2, Related to Figure 3.

Figure S3. Comparison of the proximity labelling map with published interactome data of SARS-CoV-2, Related to Figure 3.

Figure S4. Integration analysis of the proximity labelling map with multi-omics data of SARS-CoV-2, Related to Figure 3.

Figure S5. NSP14 and NSP16 block the IFN signalling through the Hippo pathway, Related to Figure 3.

Figure S6. The drugs have no antiviral activities against SARS-CoV-2, Related to Figure 7.

Figure S7. Comparison of the proximity labelling map with other studies of SARS-CoV-2, Related to Figure 3.

Table S1. SARS-CoV-2 proteins used in the proximity labelling experiments and top 5th percentile of non-specific co-purified proteins, Related to Figure 1.

Table S2. The original identified proteins by LC-MS/MS, the proximal human proteins of SARS-CoV-2 and the number of proximal proteins for each protein of SARS-CoV-2, Related to Figure 3.

Table S3. The results of the Gene Ontology and Reactome pathways over-representation analysis, Related to Figure 3.

Table S4. Integration analysis of the proximity labelling map and multi-omics data of SARS-CoV-2, Related to Figure 3.

Table S5. Potential targets and drugs revealed by the SARS-CoV-2 proximity labelling map, Related to Figure 7.

Table S6. Oligonucleotides used in this study, Related to STAR Methods.

Data S1. Proximal proteins network for individual proteins of SARS-CoV-2, Related to Figure 3.

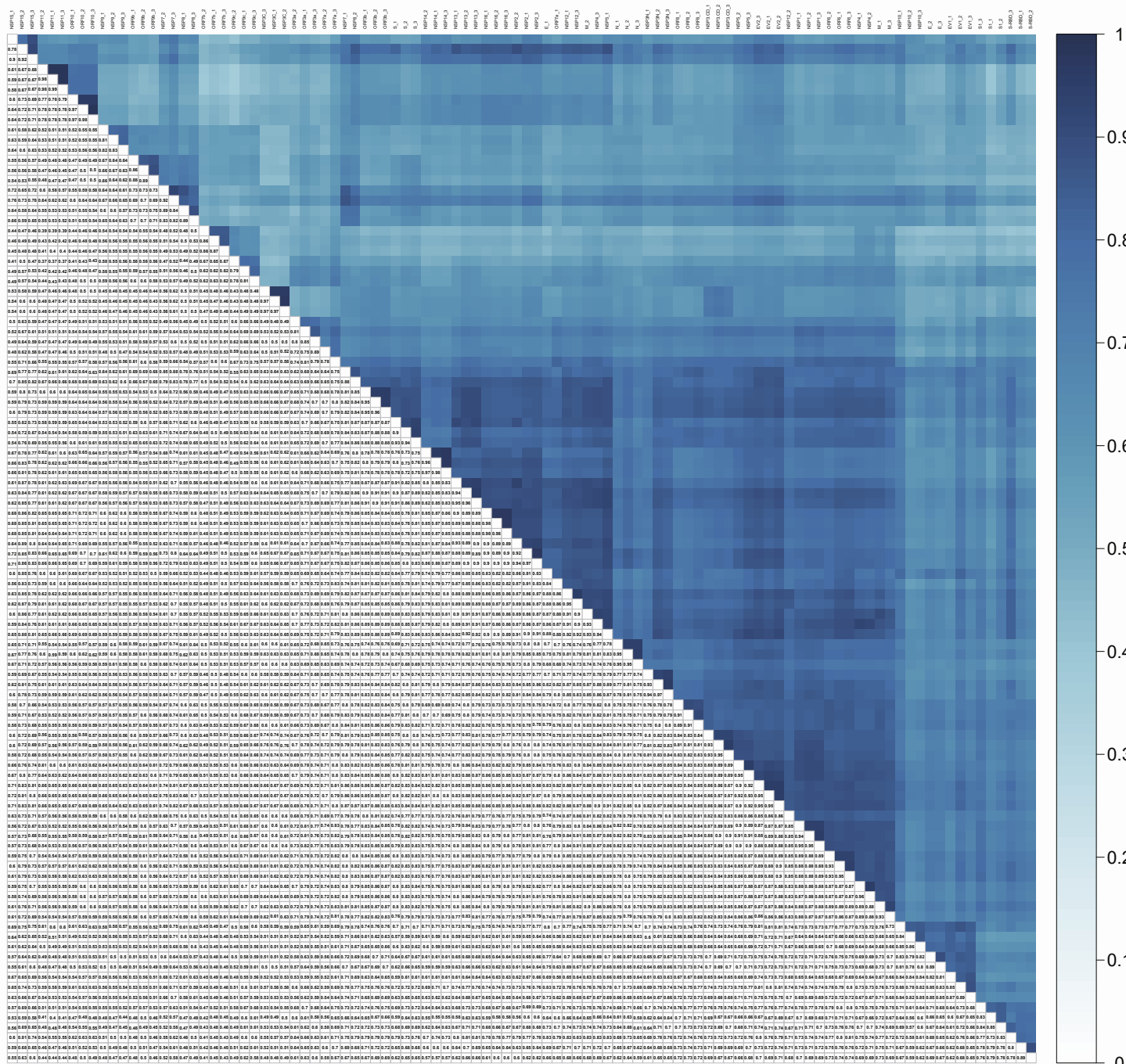


Figure S1. Correlation analysis of each sample of the proximity labelling experiments, Related to Figure 3. For each SARS-CoV-2 protein sample, Pearson's correlation coefficients of three biological replicates were clustered and visualized by Corplot (<https://github.com/taiyun/corplot>).

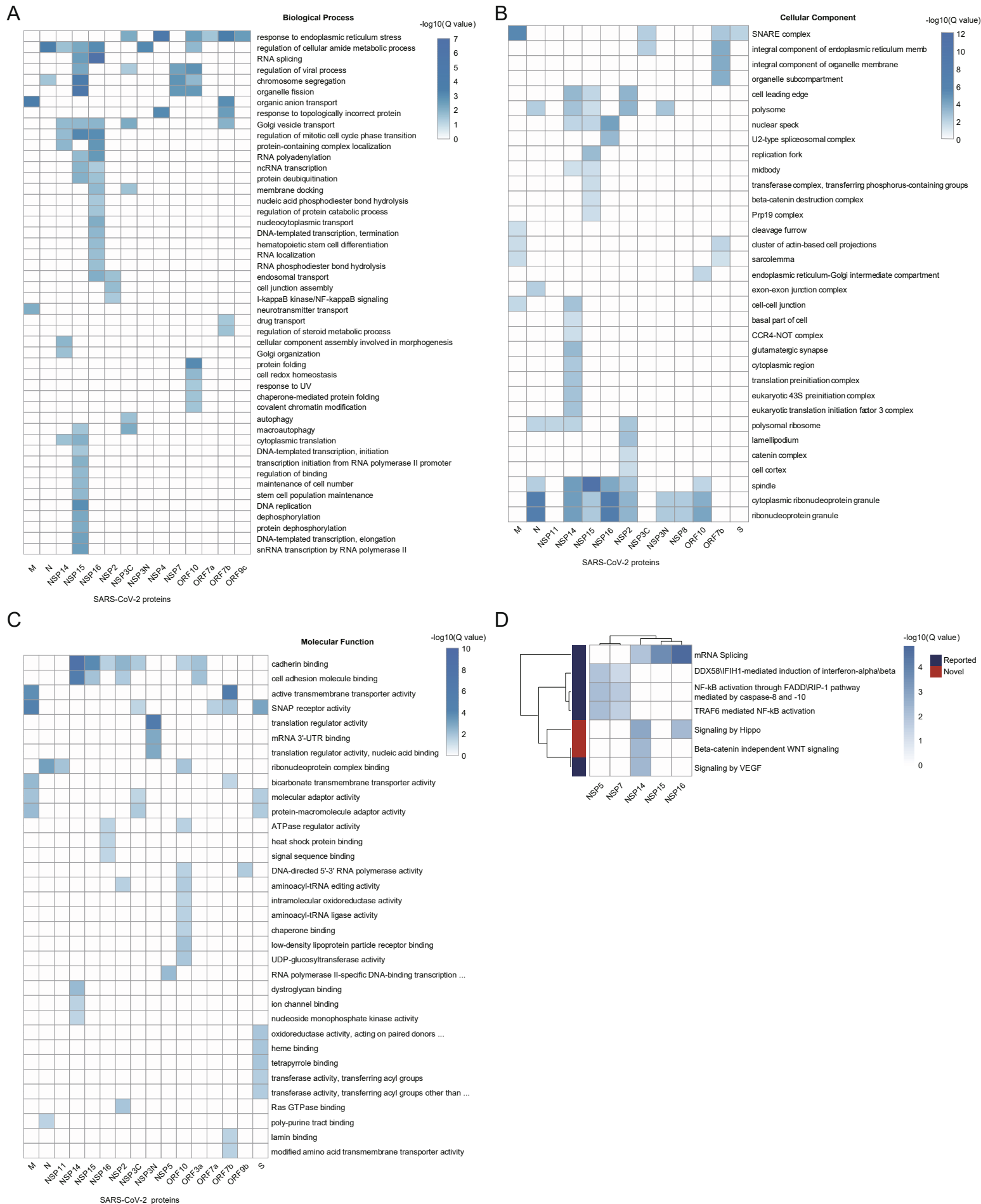


Figure S2. Gene Ontology (GO) and pathway (Reactome) analysis of the proximal proteins of SARS-CoV-2, Related to Figure 3. The proximal proteins of each viral protein were analysed using clusterProfiler. GO terms or pathways with Q-values less than 0.05 were considered significantly enriched. Redundant GO terms were reduced by REViGO for visualization, including biological processes (Figure S2A), cellular components (Figure S2B), and molecular functions (Figure S2C). The selected pathways of interest were shown (Figure S2D).

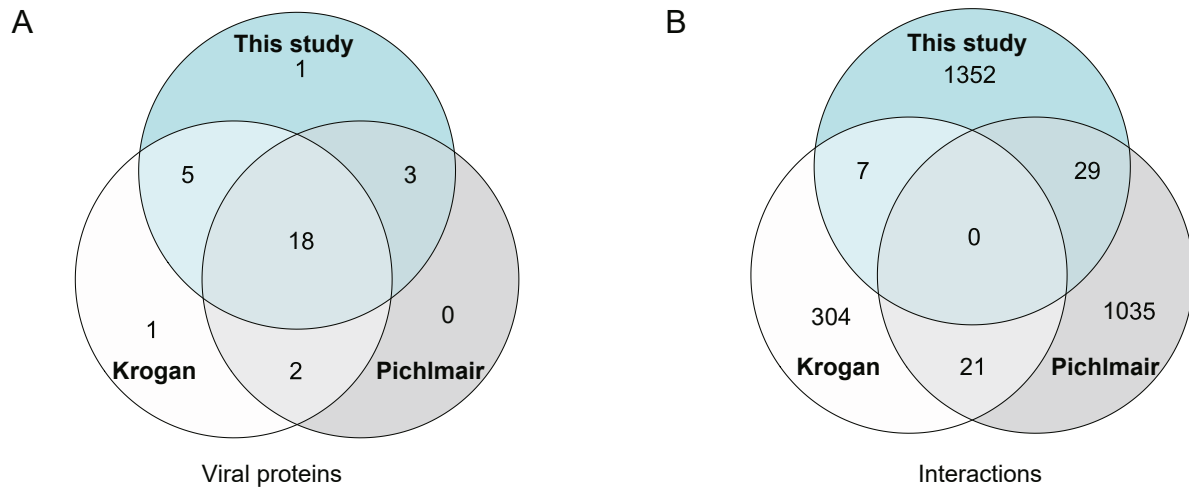


Figure S3. Comparison of the proximity labelling map with published interactome data of SARS-CoV-2, Related to Figure 3. (A) Venn diagram of viral proteins in the final interactome lists of the three groups. (B) Venn diagram of the interactions among the lists of the three groups.

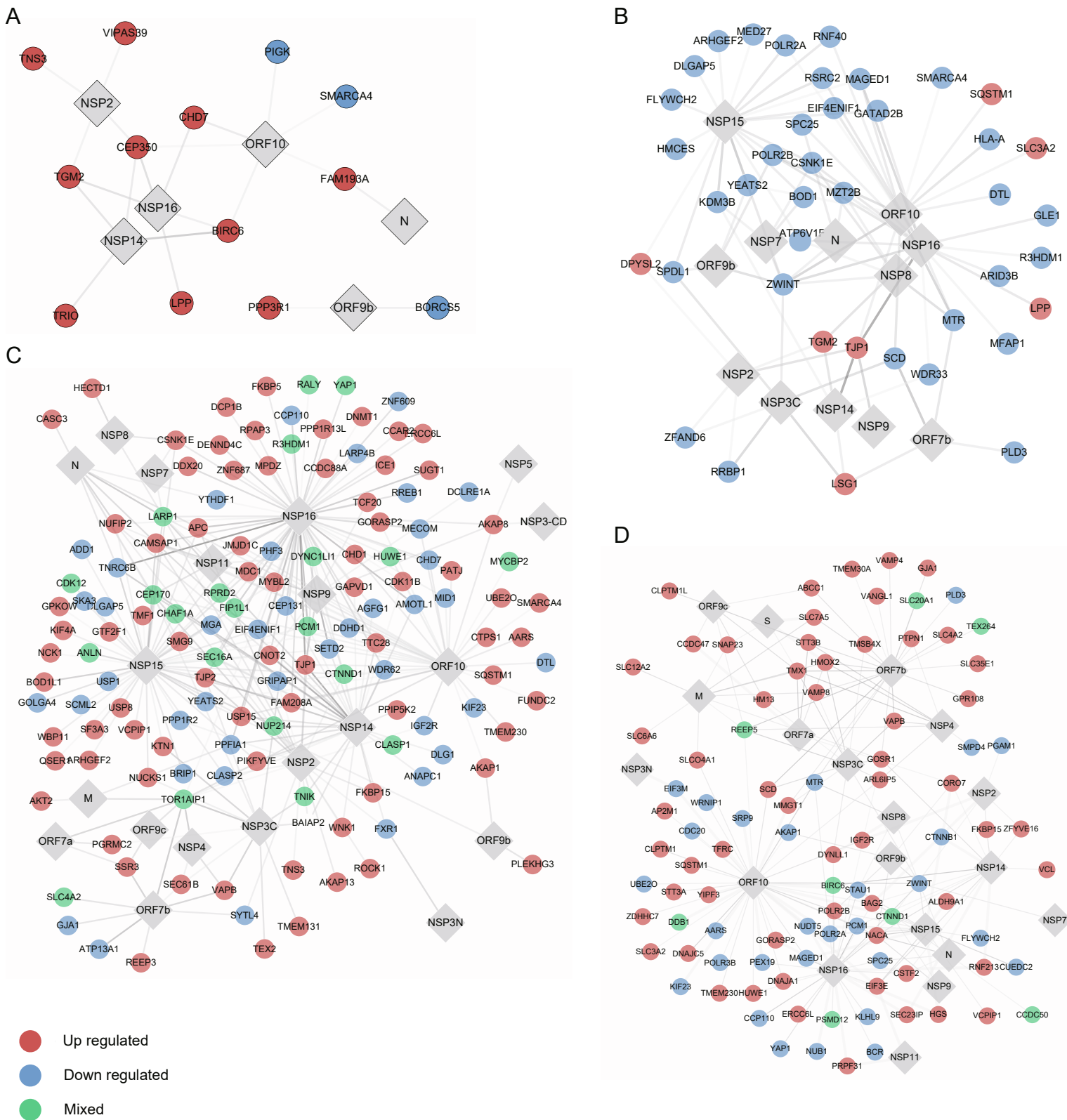


Figure S4. Integration analysis of the proximity labelling map with multi-omics data of SARS-CoV-2, Related to Figure 3. The proximal proteins were mapped to the transcriptome (Figure S4A), proteome (Figure S4B), phosphoproteome (Figure S4C) and ubiquitinome (Figure S4D) after SARS-CoV-2 infection.

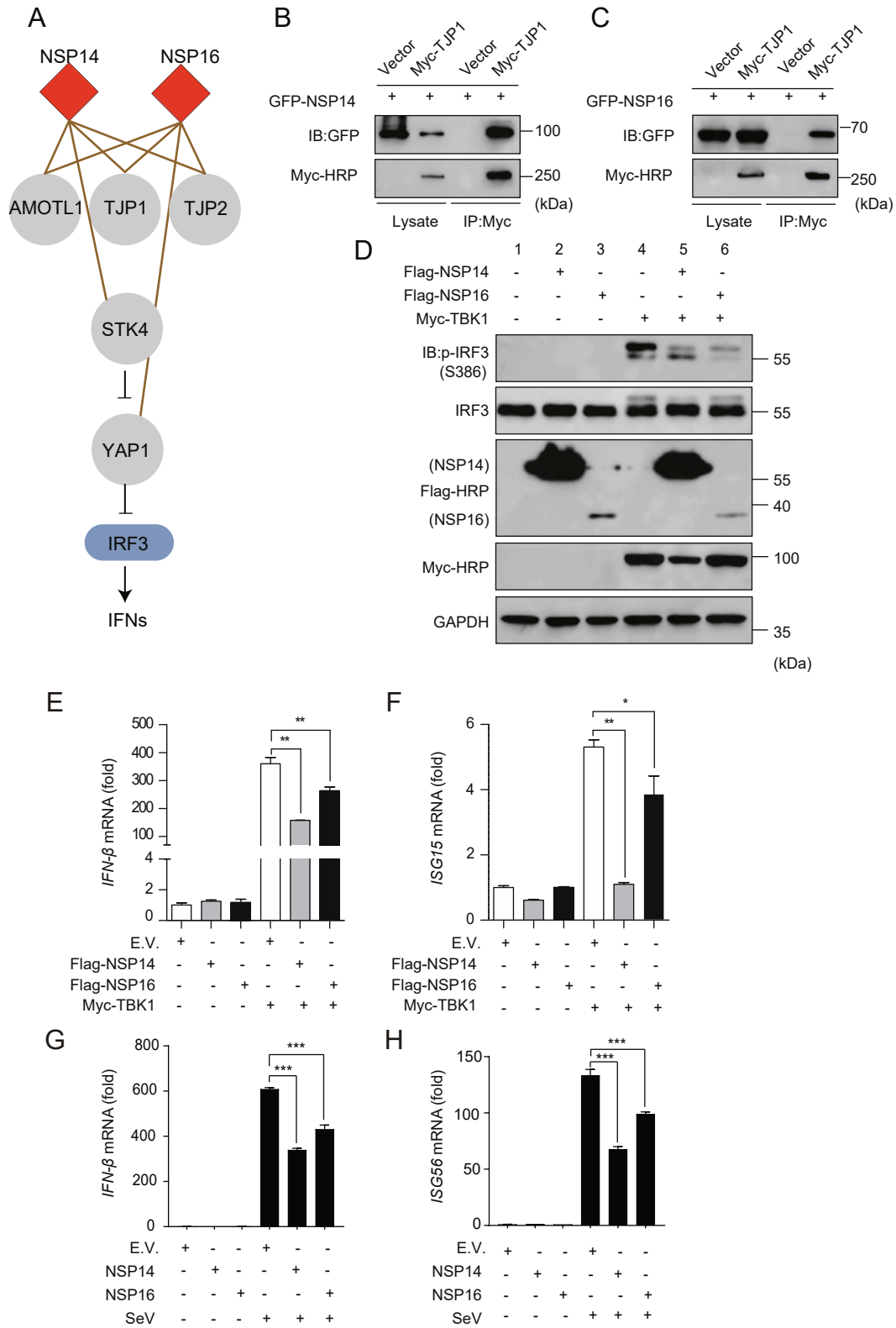


Figure S5. NSP14 and NSP16 block the IFN signalling through the Hippo pathway, Related to Figure 3. (A) The Hippo signalling pathway is associated with NSP14 and NSP16. (B, C) Validation of the interactions of NSP14, NSP16 and TJP1 by co-immunoprecipitation assay. HEK293T cells were co-transfected with the indicated vectors and detected by Myc or GFP antibodies. (D) HEK293T cells were transfected with Myc-TBK1 together with empty vector or Flag-NSP14/16. phospho-Ser386 and total IRF3, NSP14, NSP16, TBK1 and GAPDH were detected by the indicated antibodies. (E, F) HEK293T cells were treated as in (D). The induction of IFN-β and ISG15 was measured by RT-qPCR. (G, H) HEK293T cells were transfected with the indicated plasmids. 24 h later, the cells were infected with SeV (50 HA/mL) as indicated. 6 h post-infection, the cells were harvested for RNA isolation. The induction of IFN-β and ISG56 was evaluated by RT-qPCR. GAPDH was used as an internal control. The fold changes were quantified by the 2-ΔΔCt method. *p < 0.05, **p < 0.01, ***p < 0.001 (two-tailed Student's t-test), means + SD, n = 3. Data are representative of two (B-D) or three (E-H) independent experiments. E.V., empty vector.

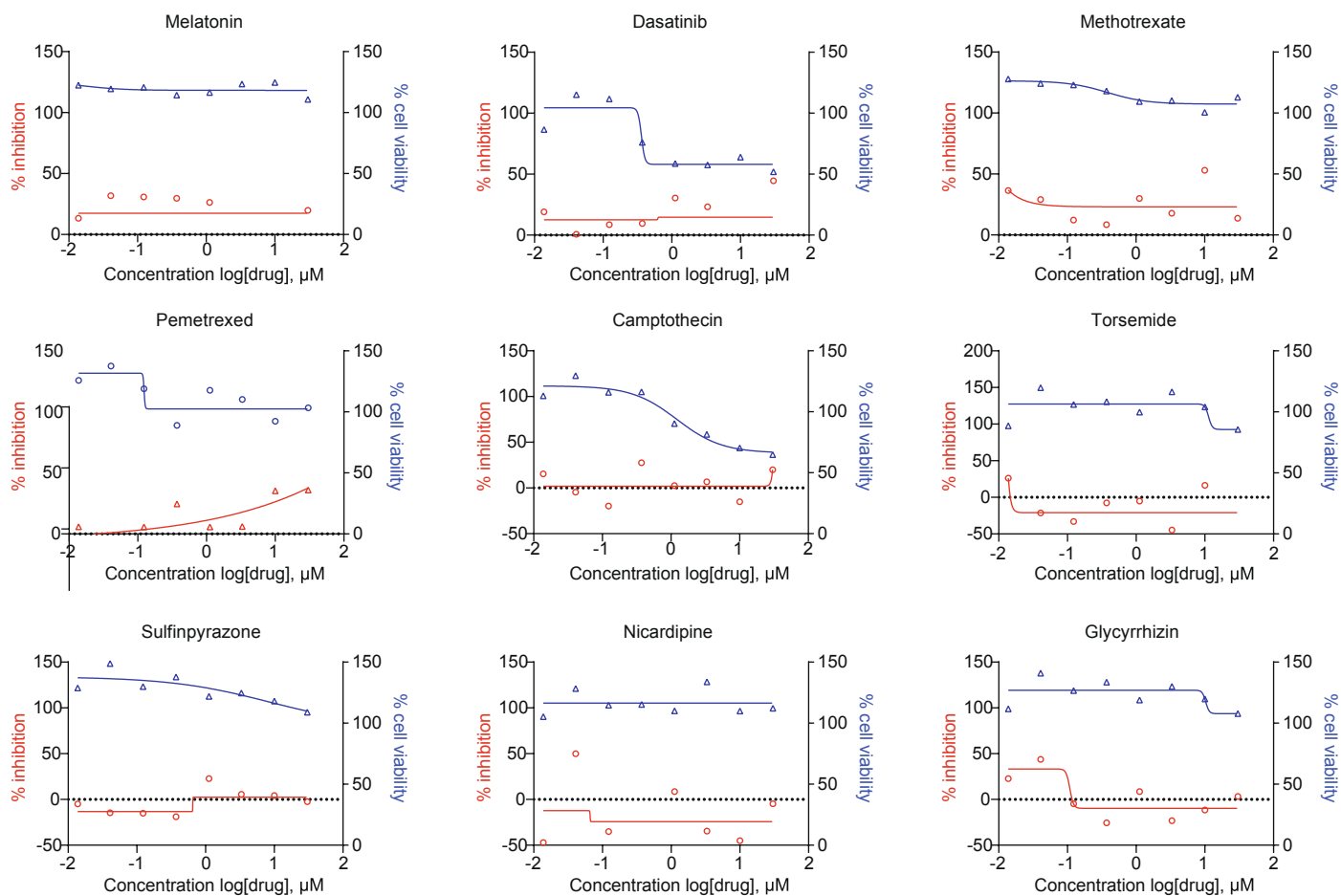


Figure S6. The drugs have no antiviral activities against SARS-CoV-2, Related to Figure 7. Vero E6 cells were seeded in 96-well plates one day before infection. For IC₅₀ determination, the cells were pre-treated with drugs for 1 h at gradient concentrations. After 48 h, supernatants were harvested for RNA extraction. Then, the viral N mRNA was quantified by RT-qPCR, and the inhibition ratio was calculated. Cell viability was evaluated by using a CCK8 kit. Red, percentage of inhibition; Blue, cell viability. Data are representative of two independent experiments (n=2).

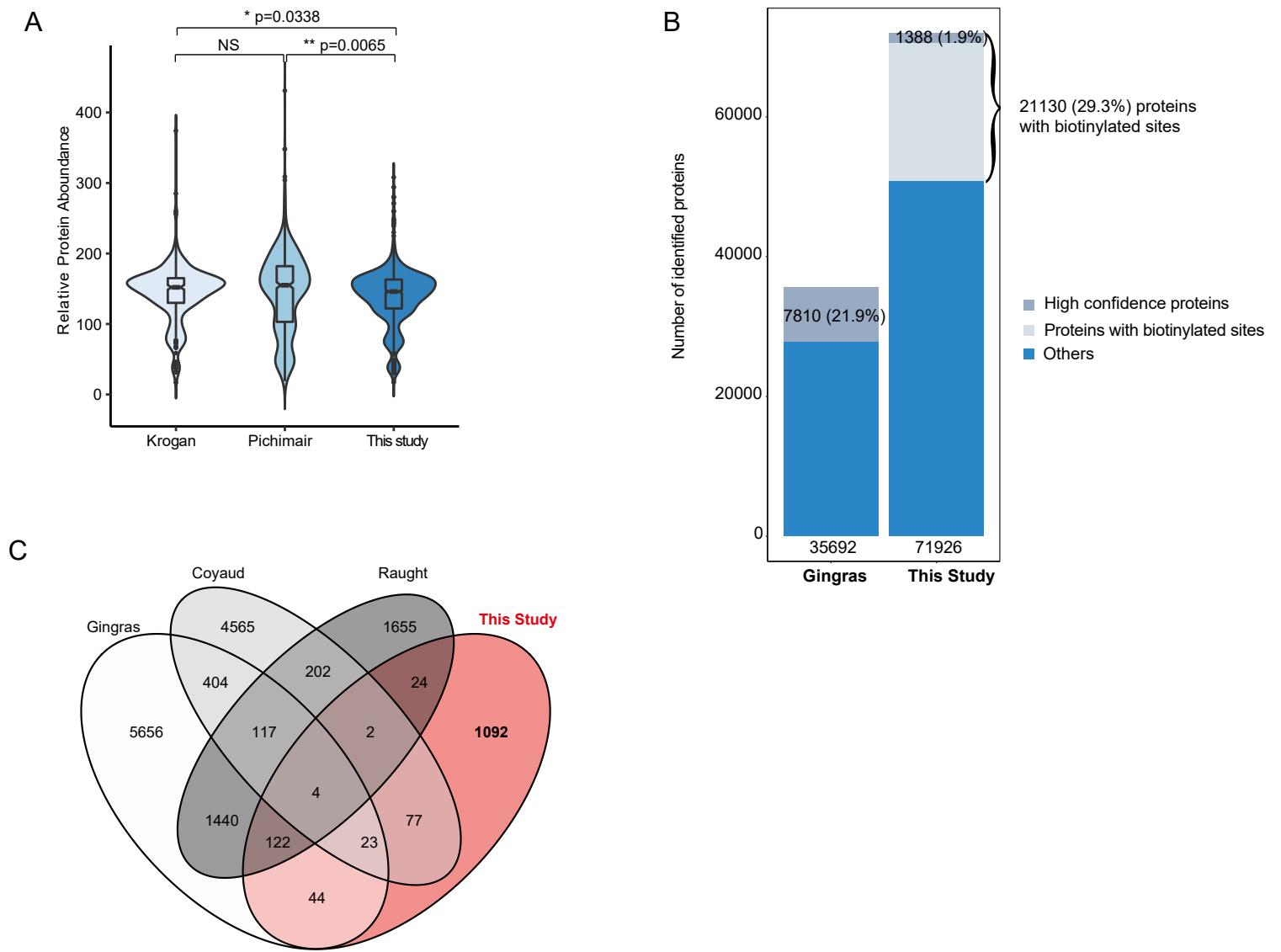


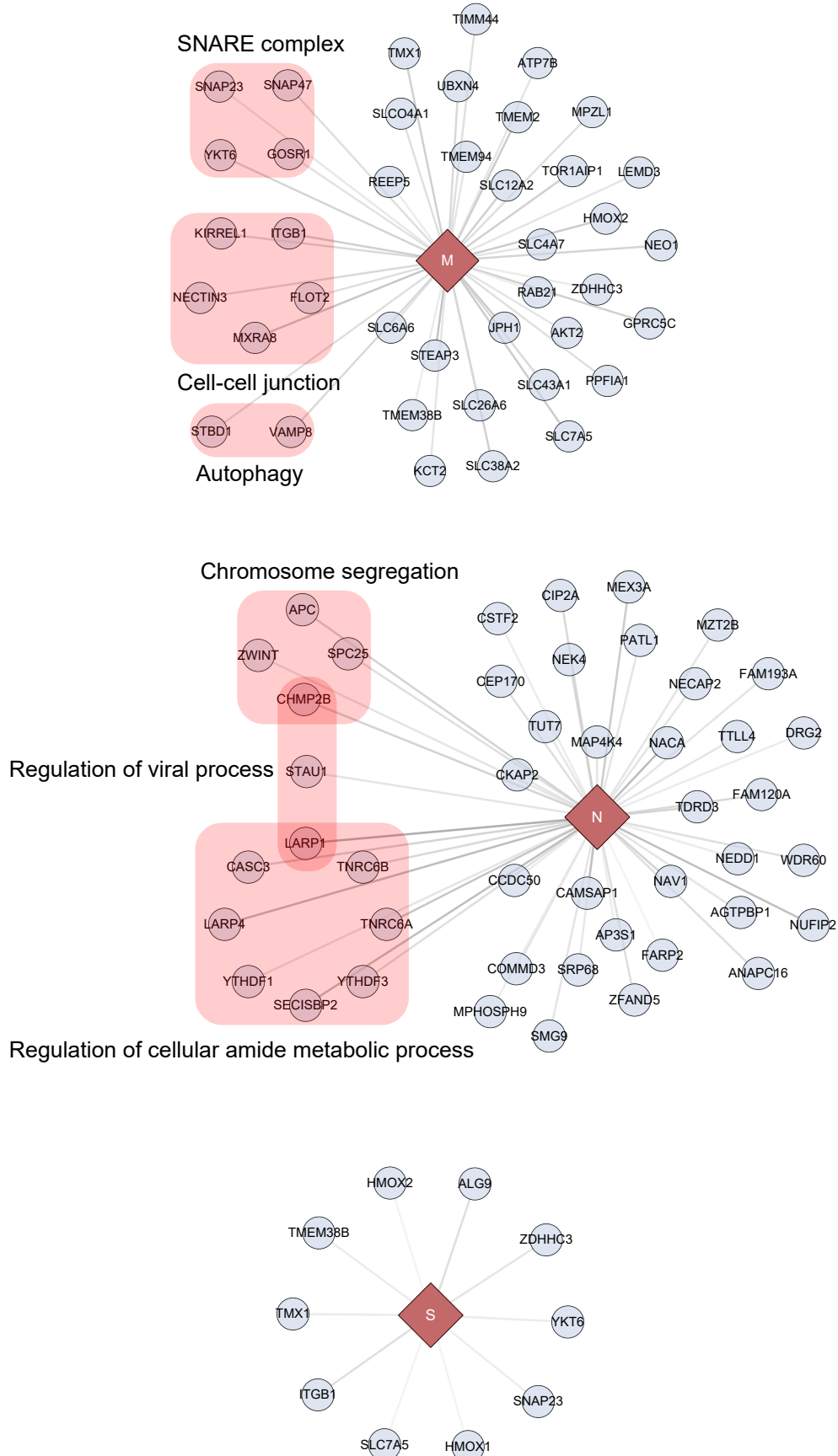
Figure S7. Comparison of the proximity labelling map with other studies of SARS-CoV-2, Related to Figure 3. (A) The abundance of interacting proteins from two studies (Krogan et al. Nature, 2020, 583(7 816):459-468; Pichimair et al. Nature, 2021, doi: 10.1038/s41586-021-03493-4) and this study was compared. The relative protein abundance data in HEK293T and A549 cell lines were obtained from the PaxDB database (Proteomics. 2015, 15(18):3163-8.). Error bars, SD. * $p < 0.05$, ** $p < 0.01$ (Student's t test). NS, not significant. (B) Comparison of the original data from Gingras's data (bioRxiv, 2020.2009.2003.282103.) and this study. This study identified that 29.3% of proteins had biotinylated sites. We finally identified 1388 proximal proteins (1.9%) with high confidence. (C) Comparison of the proximity labelling map with other proximity-dependent labelling studies of SARS-CoV-2. Venn diagram of interactions among the lists of our study and three other proximity-dependent labelling studies of SARS-CoV-2 reported by Gingras, Coyaud and Raught.

Table S6. Oligonucleotides used in this study, Related to STAR Methods.

REAGENT or RESOURCE	SOURCE	IDENTIFIER
Oligonucleotides		
scrambled control RNA-siRNA: 5'- UUCUCCGAACGUGUCACGUTT-3'(sense)	Genepharma	N/A
<i>Setd2</i> -siRNA: 5'-GCUCAGAGUUAACGUUUGA-3' (sense)	Genepharma	N/A
<i>Itgb1</i> -siRNA1: 5'-GAACAGAUCUGAUGAAUGATT- 3' (sense)	Genepharma	N/A
<i>Itgb1</i> siRNA2: 5'-GAUCAUUGAUGCAUACAAUTT- 3' (sense)	Genepharma	N/A
<i>Itgb1</i> siRNA3: 5'- GUGGUUUCGAUGCCAUCAUTT- 3' (sense)	Genepharma	N/A
Primer-Human <i>IFN-β</i> (Fw): 5'- CCAACAAGTGTCTCCTCCAAAT-3'	Synbio Technologies	N/A
Primer-Human <i>IFN-β</i> (Rev): 5'- AATCTCCTCAGGGATGTCAAAGT-3'	Synbio Technologies	N/A
Primer-Human <i>ISG15</i> (Fw): 5'- GGACAAATGCGACGAACC-3'	Synbio Technologies	N/A
Primer-Human <i>ISG15</i> (Rev): 5'- CCCGCTCACTTGCTGCTT-3'	Synbio Technologies	N/A
Primer-Human <i>GAPDH</i> (Fw): 5'- AGGGCTGCTTTTAACTCTGGT-3'	Synbio Technologies	N/A
Primer-Human <i>GAPDH</i> (Rev): 5'- CCCCACTTGATTTTGGAGGGA-3'	Synbio Technologies	N/A
Primer-Human <i>ISG54</i> (Fw): 5'- CTGCAACCATGAGTGAGAA-3'	Sangon Biotech	N/A
Primer-Human <i>ISG54</i> (Rev): 5'- CCTTTGAGGTGCTTTAGATAG-3'	Sangon Biotech	N/A

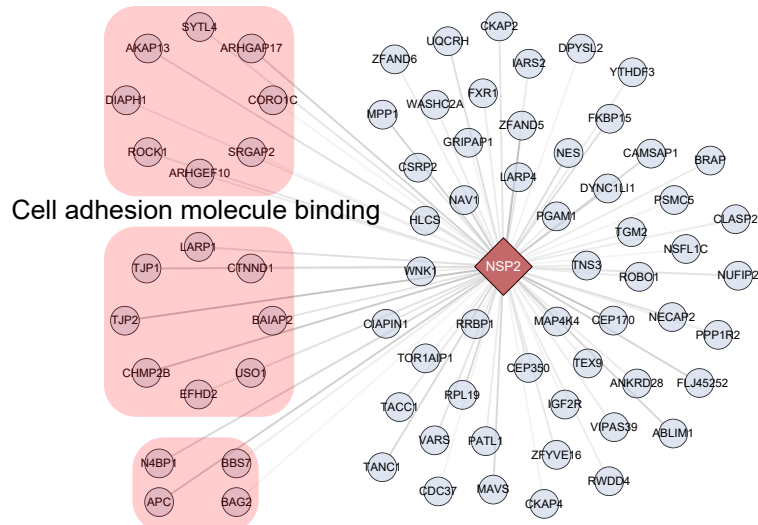
Primer-Human <i>ISG56</i> (Fw): 5'- TACAGCAACCATGAGTACAA'	Sangon Biotech	N/A
Primer-Human <i>ISG56</i> (Rev): 5'- TCAGGTGTTTCACATAGGC-3'	Sangon Biotech	N/A
Primer-Human <i>GAPDH</i> (Fw): 5'- CGGAGTCAACGGATTTGGTCGTA-3'	Sangon Biotech	N/A
Primer-Human <i>GAPDH</i> (Rev): 5'- AGCCTTCTCCATGGTGGTGAAGAC-3'	Sangon Biotech	N/A
Primer-Human β - <i>actin</i> (Fw): 5'- GGATGCAGAAGGAGATCACTG-3'	Sangon Biotech	N/A
Primer-Human β - <i>actin</i> (Rev): 5'- CAAGTACTCCGTGTGGATCG-3'	Sangon Biotech	N/A

Structrual Protein(M, N, S)



Non Structural Proteins (NSP2, NSP3C, NSP3N, NSP4)

Ras GTPase binding



Cell adhesion molecule binding

Regulation of protein catabolic process

Regulation of viral process

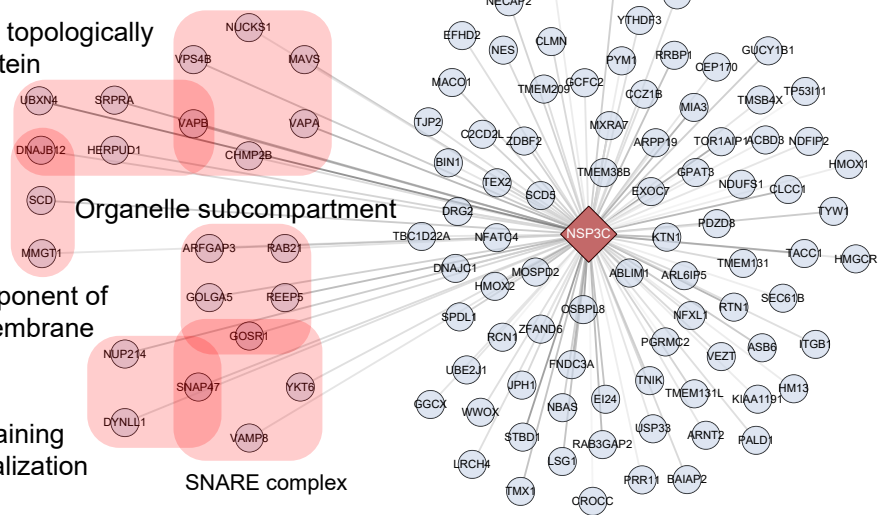
Response to topologically incorrect protein

Organelle subcompartment

Integral component of organelle membrane

Protein-containing complex localization

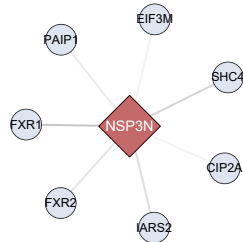
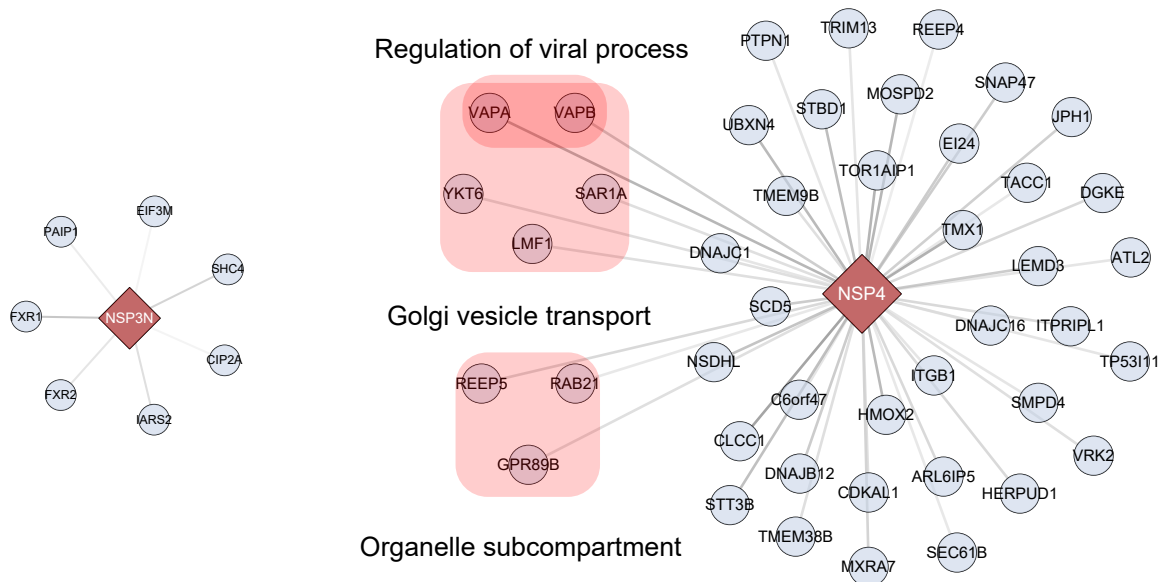
SNARE complex



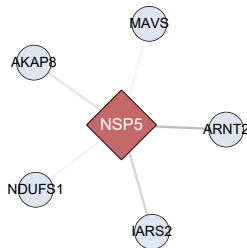
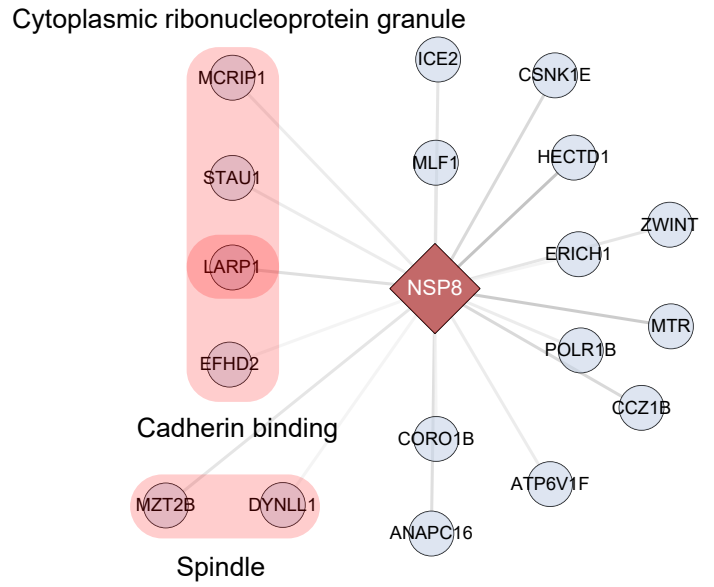
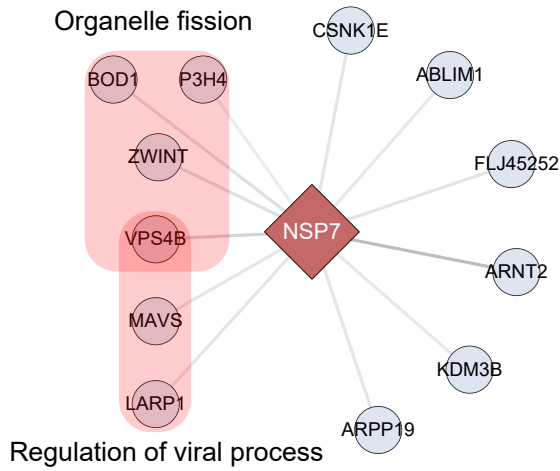
Regulation of viral process

Golgi vesicle transport

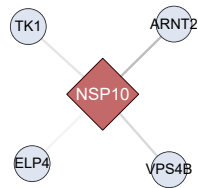
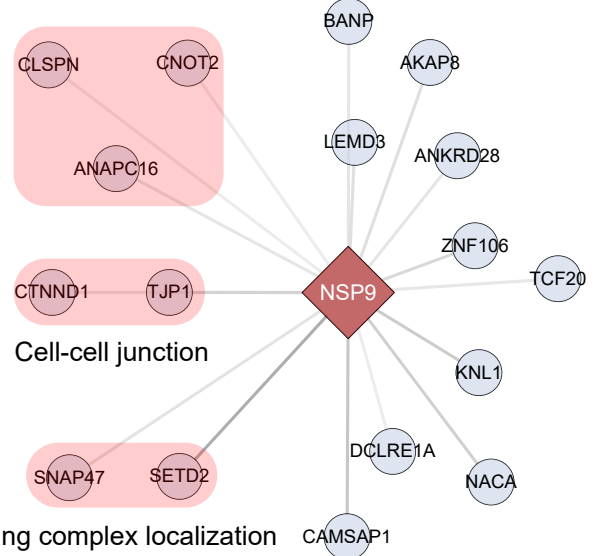
Organelle subcompartment



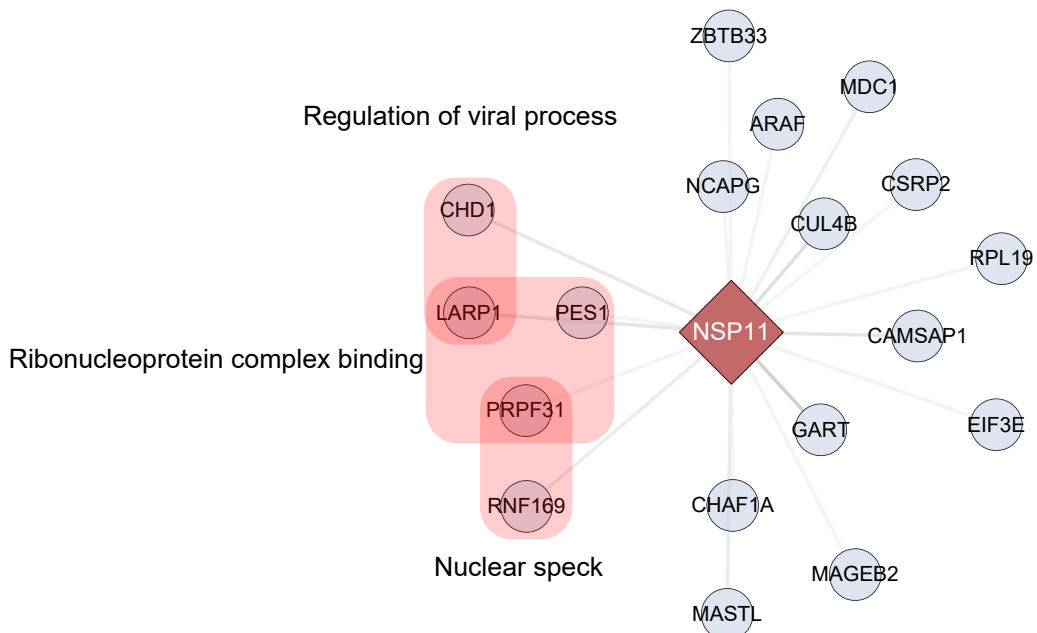
Non Structural Proteins (NSP5, NSP7, NSP8, NSP9, NSP10, NSP11)



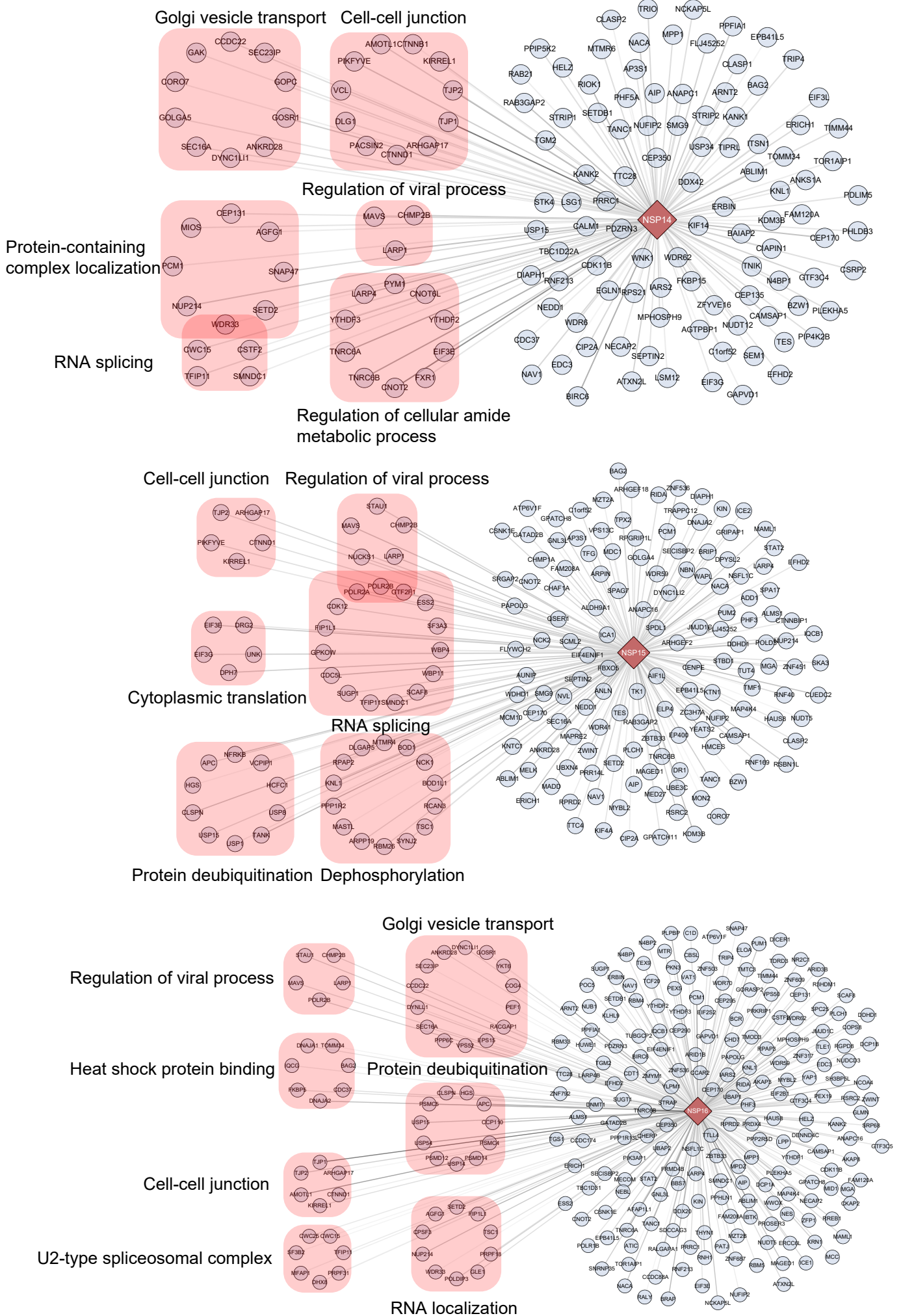
Regulation of mitotic cell cycle phase transition



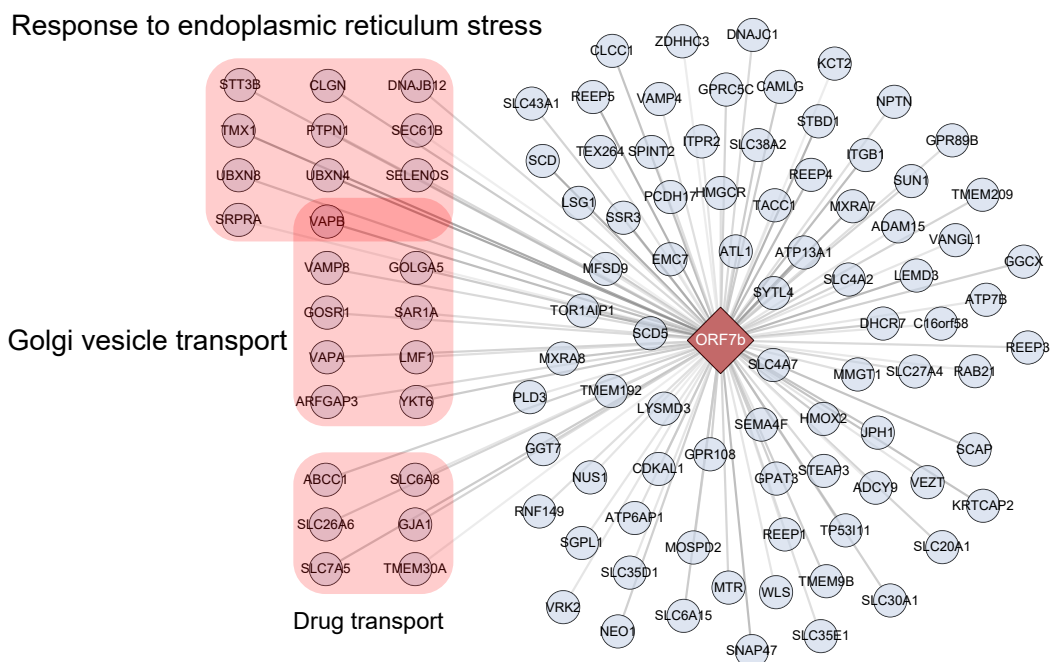
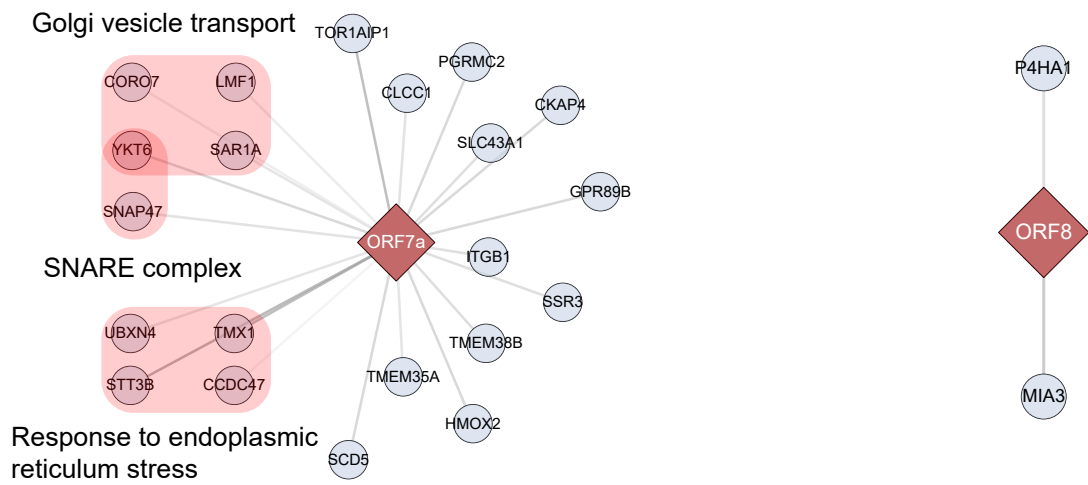
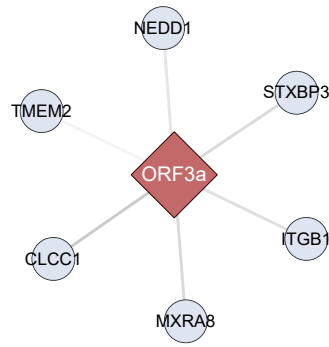
Regulation of viral process



Non Structural Proteins (NSP14, NSP15, NSP16)



Accessory proteins (ORF3a, ORF7a, ORF7b, ORF8)



Accessory proteins (ORF9b, ORF9c, ORF10)

